Journal of Neuroendocrinology, 1997, Vol. 9, 577–588

Neuroendocrine and Behavioral Responses and Brain Pattern of c-*fos* Induction Associated with Audiogenic Stress

Serge Campeau and Stanley J. Watson
Mental Health Research Institute, The University of Michigan, 205 Zina Pitcher Place, Ann Arbor, MI 48109, USA.

Key words: activity, auditory, histochemistry, corticosterone, noise, rat.

Abstract

The present study determined simultaneously the behavioural, neuroendocrine and regional brain activity, using semi-quantitative analysis of c-*fos* mRNA induction, produced by 30 min of auditory stimulation at different white noise intensities (background 60 dB, 70, 80, 90 and 105 dBA), in rats. Only the highest noise intensities (90 and 105 dB) significantly increased corticosterone release after 30 min stimulation. Behaviourally, the 105 dB noise condition reliably reduced overall activity, and moderate noise intensities (70 and 80 dB) increased sleeping time. Three distinct patterns of c-*fos* mRNA induction were observed. First, following exposure to the experimental cages, a wide pattern of brain activation was obtained in experimental animals irrespective of noise intensity presentation, compared to the naive rats. Second, a number of auditory structures (cochlear nuclei, superior olivary complex, nuclei of the lateral lemniscus, inferior colliculus and the medial division of the medial geniculate body) displayed a clear intensity-dependent increase in c-*fos* induction. Third, compared to all other conditions, the stressed rats (90 and 105 dB conditions) displayed significantly higher c-*fos* induction in relatively few areas. Particularly intense c-*fos* induction was observed in the bed nucleus of the stria terminalis, especially its anterior medial and ventral aspects, the septohypothalamic nucleus, the ventral lateral septum, the ventral portion of the dentate gyrus, a number of hypothalamic nuclei including the lateral preoptic area, the medial preoptic nucleus and the paraventricular nucleus, the median raphe and the pedunculopontine tegmental nucleus. The involvement of a number of these structures in a specific audiogenic stress responsive circuit is discussed.

Recently, immediate-early genes (e.g. c-*fos*, c-*jun*, *zif*/268) have been used as neuroanatomical markers to determine the pattern of brain activity and neural pathways associated with a variety of stressors (1–14). The few detailed and quantitative analyses of immediate-early gene expression have revealed that physical or psychological stressors (restraint/immobilization, forced swim and fear) appear to activate a large number of brain areas (1, 11). Because many brain areas were commonly activated by the above stressors, these regions have been proposed to underlie a neural system reflecting a general state of stress. However, this conclusion might be premature because most of the above stress conditions cannot be controlled easily, and therefore, some of the regional activity detected might reflect processes that are not specific to the specific stress stimuli employed.

The main goal of the present study was to use increasing intensities of white noise to determine the specific brain areas, using semi-quantitative analysis of the immediate early gene c-*fos*, involved in audiogenic stress. Acoustic stimulation, which can be graded from non-stress to stressful levels, was used to help control for processes other than those directly responsible for audiogenic stress. To determine the stressful nature of increasing auditory stimulation, the levels of plasma corticosterone were measured, as a reliable index of hypothalamo-pituitary-adrenal activation induced by a variety of stressful conditions, including loud auditory stimulation (15–21). In addition, behaviour was monitored since previous studies have established that overall activity is reliably reduced by loud noise stimulation (19–21). The data obtained indicate that a limited number of brain regions are selectively activated in rats stressed with loud noise, as measured with c-*fos* mRNA induction.

Results

Plasma corticosterone release evoked by the exposure of rats to 30 min of white noise at various intensities, or in naive control rats, is presented in Fig. 1. One-way ANOVA revealed a significant effect of the different noise intensities, $F(5,18) = 18.87$, $P < 0.001$. Post-hoc multiple mean comparisons (Tukey) indicated that rats from the 2 higher noise intensity groups (90 and 105 dB) had significantly higher plasma corticosterone levels compared to all other groups, but were not different from each other ($P < 0.05$). No other differences were obtained.

The behaviour of rats from the different noise intensity conditions also showed reliable differences, as shown in Fig. 2. Mean

Correspondence to: Serge Campeau, Mental Health Research Institute, The University of Michigan, 205 Zina Pitcher Place, Ann Arbor, MI 48109–0720, USA.

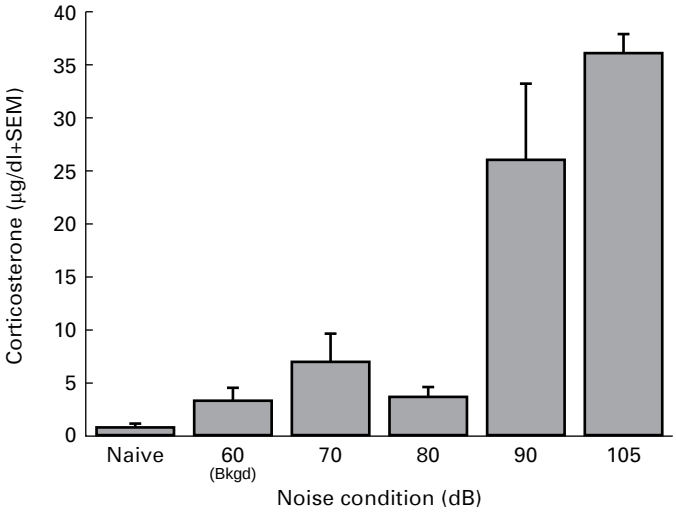

FIG. 1. Plasma corticosterone values (μg/dl + SEM) in each of the noise conditions obtained from trunk blood 30 min following initiation of noises at the different intensities or after cage placement (60 dB Bkgd), or immediately upon removal from the home cages (Naive).

immobility scores were reliably different between the various noise intensity conditions, $F(4,15)=5.42$, $P<0.01$, particularly for the last 20 min. Multiple mean comparisons indicated that rats from the 105 dB condition were more immobile than rats from other conditions, especially during the last time period. Total active behaviours (sum of locomotion, rearing and grooming behaviours) were also reliably different over the entire noise session, $F(4,15)=4.41$, $P<0.05$, particularly during the last 20 min. This was mainly due to lower overall activity from rats in the 105 dB condition. The reduced active behaviours observed in the 70 and 80 dB conditions could be attributed to increased sleeping time in those groups, as revealed by a significant Condition × Time period interaction, $F(20,75)=2.59$, $P<0.005$. Rats from the 70 and 80 dB groups displayed significantly more sleeping during the last time period (25–30 min) than any other group, $F(4,15)=12.35$, $P<0.001$, but were not different from each other.

C-*fos* mRNA was widely induced in the brains of rats decapitated 30 min following the beginning of different noise intensity conditions, as measured by semi-quantitative integrated densitometric measurements from x-ray films presented in Table 1. A majority (65) of the 71 brain regions analysed displayed reliable c-*fos* induction in one or more of the experimental conditions, compared to the naive rats (ANOVAs, $P<0.05$). Representative examples of c-*fos* induction in the naive, 60, 80 and 105 dB conditions are presented at eight levels of the neuraxis in Figures 3 and 4.

Many of the regions (31) quantified displayed c-*fos* induction above naive levels, irrespective of noise intensity. Thus, simply placing rats in the experimental boxes in which they had previously been exposed for nine days (60 dB background condition) was sufficient to reliably induce c-*fos* in many brain areas that was not statistically exceeded by presentation of louder noise intensities (up to 105 dB, see Table 1). This was notable in the amygdala, thalamus and cortex, and a few additional structures in the hippocampus, midbrain, pons and brainstem. This is depicted in Fig. 5 for some areas in standardized scores (z) from the raw integrated densities. Presentation of white noise 10 or 20 dB above background level (70 and 80 dB conditions, respectively) produced a pattern of c-*fos* induction remarkably similar to the 60 dB background noise condition, except for moderately higher induction in some auditory areas.

Many auditory areas, including the cochlear nuclei, superior olivary complex, nuclei of the lateral lemniscus, external nucleus of the inferior colliculus and the medial division of the medial geniculate body, showed increasing c-*fos* induction with increasing noise intensities. Figure 6 illustrates all the auditory areas measured and the intensity-dependent c-*fos* induction relationship obtained in many of these areas.

Exposure of rats to noise intensities (90 and/or 105 dB noise conditions) which evoked reliable corticosterone release, resulted in additional but limited regional c-*fos* induction that was significantly greater than that observed in rats from all other groups (Naive, 60, 70 and 80 dB). These regions, depicted in Fig. 7, included the anterior bed nucleus of the stria terminalis (medial and ventral), septohypothalamic nucleus, ventral dentate gyrus, lateral preoptic area, medial preoptic and paraventricular nuclei of the hypothalamus, median raphe and the pedunculopontine tegmental nucleus. Four brain areas from rats in the 90 and/or 105 dB conditions displayed reliable c-*fos* induction compared to the Naive, 60 dB background and 70 dB conditions; the lateral septum (ventral), supramammillary nucleus, laterodorsal central gray and the central/dorsal nuclei of the inferior colliculus. The lateral nucleus of the amygdala, the superior colliculus and the laterodorsal tegmental nucleus from rats in the 90 and/or 105 dB conditions showed higher c-*fos* induction compared to the Naive and 60 dB background conditions. Six additional brain areas from rats in the 90 and/or 105 dB conditions, namely the nucleus accumbens (mostly shell), ventromedial nucleus of the hypothalamus, ventral posterior and oculomotor nuclei of the thalamus, dorsal raphe and the dorsal tegmental nucleus, showed reliable c-*fos* induction only compared to Naive rats. The auditory nuclei of the lateral lemniscus were the only regions in which c-*fos* induction between the 90 and 105 dB conditions was reliably different.

Discussion

Exposing rats to white noise intensity levels of 90 dB or greater reliably evoked the release of corticosterone, as reported previously with loud auditory stimulation (15–21). The present results, however, offer the first clear demonstration of a noise intensity dependent corticosterone release function, with a threshold for activation at ≈90 dB (30 dB above background noise levels). The reduced behavioural activity of rats exposed to the highest noise intensity (105 dB) is also consistent with the results of prior studies (19–21), whereas the lack of behavioural inhibition to 90 dB exposure has not been reported or examined previously. This dissociation between the behavioural and neuroendocrine effects of 90 dB exposure deserves additional attention. The longer sleep duration observed particularly in rats from the 70 and 80 dB conditions provides one of the first report of experimentally induced increases in one of various sleep variables by steady state noise of moderate intensity in animals, as has been shown in newborn and adult humans (22–24).

c-*fos* was broadly induced in the brains of control rats

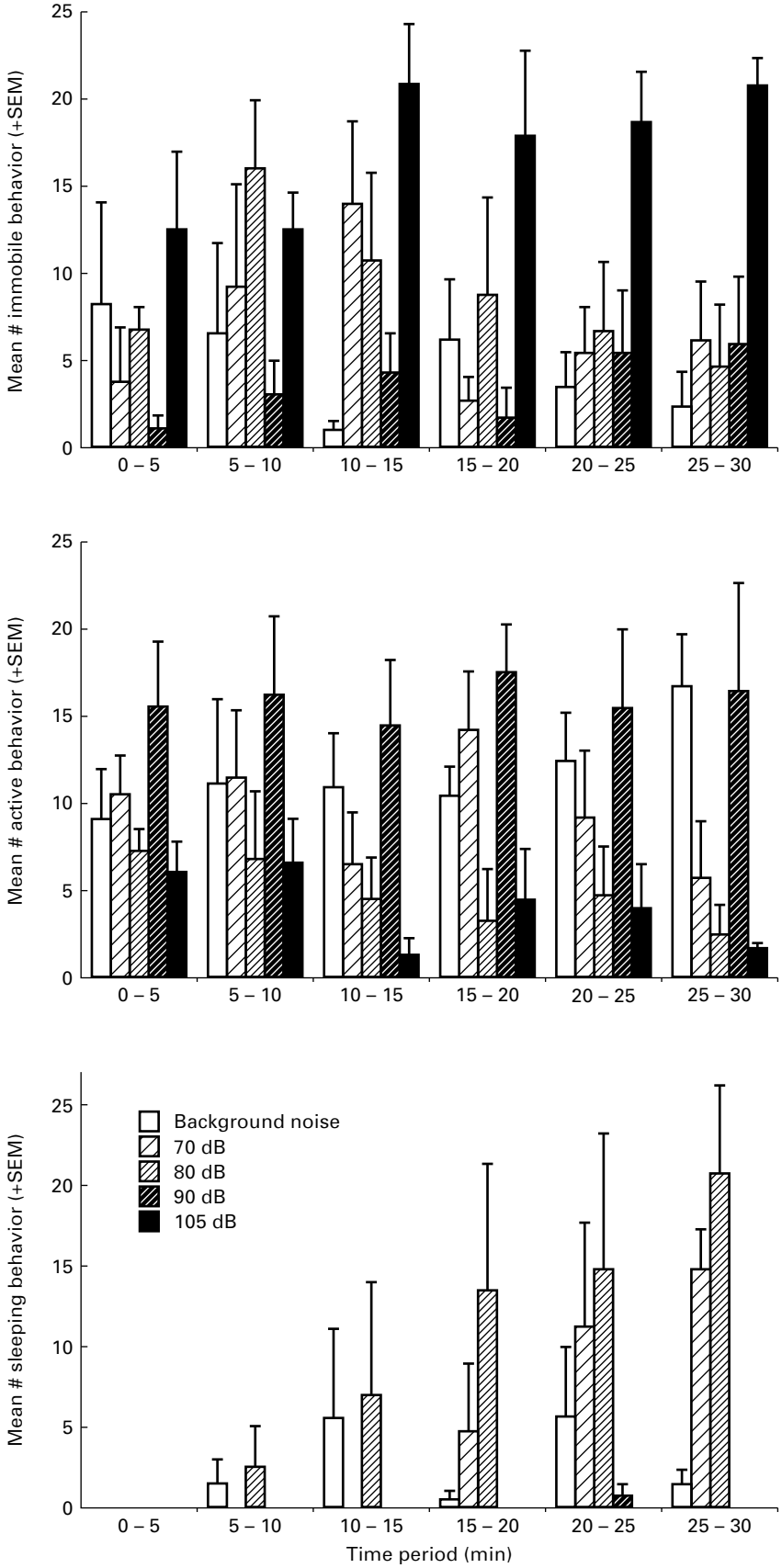

FIG. 2. Sampling of immobile (top), active (middle) and sleeping (bottom) behaviors (+SEM) in rats exposed to background noise (60), 70, 80, 90, or 105 dB.

TABLE 1. Mean Integrated Densities (/100 ± SEM).

Brain region	Experimental group											
	Naive		60 dB		70 dB		80 dB		90 dB		105 dB	
Forebrain												
Nucleus accumbens†	23	(11)	38	(15)	41	(17)	33	(14)	132[a]	(21)	159[a]	(12)
BNST medial†	0.3	(0.1)	8.3[a]	(2.0)	12[a]	(5.3)	9.6[a]	(2.2)	74[d]	(19)	99[d]	(25)
BNST ventral†	1.1	(0.6)	6.0[a]	(1.2)	5.8[a]	(1.4)	7.8[a]	(3.2)	32[a]	(6.1)	36[d]	(4.0)
Caudate nucleus dorsal†	17	(3)	134	(52)	283[a]	(208)	89	(47)	262[a]	(93)	123[a]	(21)
Caudate nucleus ventral†	5.3	(2.6)	196[a]	(165)	54	(39)	13	(5.8)	35	(14)	13	(3.7)
Dorsal endopiriform nuc†	4.6	(2.7)	64[a]	(16)	72[a]	(27)	57[a]	(14)	81[a]	(3.5)	66[a]	(4.5)
Medial septum†	1.2	(0.4)	10[a]	(3.2)	6.7[a]	(1.3)	13[a]	(7.7)	16[a]	(2.6)	13[a]	(3.3)
Lateral septum†	0.9	(0.3)	92[a]	(67)	45[a]	(18)	86[a]	(29)	448[c]	(34)	592[c]	(63)
Septohypothalamic nuc†	0.4	(0.1)	21[a]	(11)	18[a]	(6.7)	29[a]	(7.0)	182[d]	(8.2)	305[d]	(39)
Amygdala												
Anterior cortical nuclei†	14	(5.5)	95[a]	(32)	114[a]	(34)	66[a]	(15)	95[a]	(14)	108[a]	(17)
Basolateral nucleus†	12	(5.8)	53[a]	(12)	77[a]	(32)	59[a]	(11)	91[a]	(19)	74[a]	(4)
Central nucleus	14	(7.2)	6.3	(0.7)	8.8	(2.2)	10	(2.3)	11	(0.4)	17	(1.4)
Lateral nucleus†	4.8	(2.3)	24[a]	(3.8)	31[a]	(7.1)	30[a]	(4.6)	91[a]	(29)	89[b]	(5.0)
Medial nucleus†	4.0	(0.9)	50[a]	(16)	80[a]	(34)	43[a]	(13)	121[a]	(27)	59[a]	(13)
Posterior cortical nuclei†	6.2	(1.9)	133[a]	(39)	162[a]	(30)	133[a]	(37)	226[a]	(31)	215[a]	(6)
Hippocampus												
Dentate gyrus dorsal	41	(11)	41	(11)	61	(11)	43	(18)	85	(15)	42	(2.3)
Dentate gyrus ventral†	3.0	(0.6)	13	(2.9)	7.7	(2.1)	13	(6.4)	60[a]	(15)	172[d]	(49)
CA1†	5.4	(2.7)	39[a]	(2.0)	45[a]	(20)	39[a]	(11)	80[a]	(31)	39[a]	(9.7)
CA2	4.7	(2.2)	13	(1.4)	17	(8.0)	12	(2.1)	17	(4.0)	11	(3.1)
CA3†	43	(18)	117	(12)	145[a]	(44)	135[a]	(35)	185[a]	(28)	119	(11)
Cortex												
Cingulate†	107	(32)	1018[a]	(392)	1020[a]	(309)	964[a]	(347)	2101[a]	(341)	1295[a]	(135)
Enthorinal†	56	(26)	292[a]	(63)	256[a]	(58)	271[a]	(75)	382[a]	(72)	263[a]	(16)
Frontal	401	(233)	1070	(247)	768	(384)	308	(113)	941	(277)	705	(309)
Infralimbic†	11	(7.0)	223[a]	(115)	176[a]	(65)	141[a]	(57)	269[a]	(61)	221[a]	(41)
Insular	106	(32)	215	(61)	135	(56)	130	(50)	219	(43)	218	(34)
Lateralorbital†	175	(65)	1604[a]	(346)	2021[a]	(475)	1254[a]	(491)	2317[a]	(483)	1682[a]	(173)
Occipital (visual)†	619	(293)	4143[a]	(233)	4221[a]	(815)	4789[a]	(505)	6932[a]	(825)	5353[a]	(288)
Parietal†	1359	(769)	4192[a]	(781)	2549	(758)	2219	(430)	4385[a]	(1228)	3214	(873)
Perirhinal†	65	(27)	285[a]	(42)	225[a]	(72)	218[a]	(27)	461[a]	(108)	352[a]	(17)
Piriform†	240	(74)	1005[a]	(129)	1078[a]	(117)	788[a]	(133)	1267[a]	(213)	997[a]	(65)
Temporal (auditory)†	844	(257)	2166[a]	(223)	2242[a]	(345)	2496[a]	(326)	3606[a]	(227)	3731[a]	(332)
Hypothalamus												
Dorsomedial nucleus†	20	(14)	96[a]	(23)	112[a]	(42)	116[a]	(30)	284[a]	(38)	298[a]	(27)
Lateral nucleus†	15	(10)	57[a]	(14)	46	(11)	37	(13)	119[a]	(32)	104[a]	(13)
Lateral preoptic area†	2.5	(0.9)	23[a]	(15)	15[a]	(3.8)	20[a]	(6.7)	151[d]	(16)	97[c]	(27)
Medial preoptic area†	1.2	(0.4)	3.5	(1.1)	15[a]	(5.1)	9.1	(4.6)	29[a]	(15)	9.1	(2.7)
Medial preoptic nucleus†	2.1	(0.6)	31[a]	(13)	27[a]	(5.2)	35[a]	(8.8)	110[c]	(22)	166[d]	(27)
Paraventricular nucleus†	1.2	(0.6)	14[a]	(4.5)	17[a]	(4.1)	15[a]	(4.1)	102[d]	(27)	185[d]	(46)
Supramammillary nucleus†	6.6	(2.0)	65[a]	(26)	63[a]	(15)	86[a]	(30)	179[a]	(16)	302[c]	(14)
Ventromedial nucleus†	1.9	(0.7)	2.7	(0.6)	6.8	(3.9)	5.3	(1.5)	35[a]	(26)	14[a]	(0.8)
Thalamus												
Anterodorsal nucleus	48	(7.1)	97	(30)	66	(19)	54	(14)	95	(12)	96	(12)
Anteroventral nucleus†	37	(11)	315[a]	(71)	247[a]	(45)	165[a]	(16)	360[a]	(33)	269[a]	(41)
Anterior pretectal nucleus†	50	(18)	267[a]	(51)	219[a]	(57)	247[a]	(72)	342[a]	(83)	297[a]	(60)
Central nuclei†	68	(34)	351[a]	(82)	282[a]	(82)	322[a]	(56)	589[a]	(127)	489[a]	(78)
Habenula†	13	(1.9)	92[a]	(22)	58[a]	(8)	51[a]	(9)	92[a]	(17)	112[a]	(14)
Lateral posterior nuclei†	39	(18)	389[a]	(78)	297[a]	(65)	294[a]	(31)	573[a]	(85)	467[a]	(48)
Lateral geniculate†	146	(22)	701[a]	(106)	630[a]	(73)	579[a]	(96)	783[a]	(130)	646[a]	(84)
Medial geniculate medial†	3.7	(0.6)	34[a]	(6.8)	37[a]	(3.6))	56[a]	(14)	143[d]	(15)	173[d]	(3.1))
Medial geniculate ven/dor†	13	(4.2)	274[a]	(65)	279[a]	(76)	221[a]	(60)	537[a]	(64)	527[a]	(24)
Mediodorsal nucleus†	34	(17)	442[a]	(123)	452[a]	(104)	397[a]	(103)	618[a]	(122)	517[a]	(88)
Oculomotor nucleus	13	(5.3)	43	(5.9)	57	(23)	40	(21)	98[a]	(10)	80[a]	(12)
Paraventricular nucleus†	22	(4.1)	178[a]	(47)	167[a]	(41)	191[a]	(26)	331[a]	(41)	346[a]	(26)
Ventral posterior nucleus†	39	(16)	141	(30)	137	(59)	126	(46)	343[a]	(114)	262[a]	(76)
Subparafascicular nucleus†	1.8	(1.3)	33[a]	(22)	32[a]	(5.9)	54[a]	(16)	51[a]	(4.1)	152[a]	(33)
Midbrain, pons, brainstem												
Dorsolateral central gray†	1.9	(0.7)	13	(5.3)	17[a]	(7.3)	18[a]	(6.6)	111[a]	(73)	60[a]	(10)
Lateroventral central gray†	2.9	(1.3)	14	(6.6)	17[a]	(4.4)	31[a]	(10)	83[b]	(19)	127[c]	(29)
Cochlear nuclei†	20	(6.0)	73[a]	(13)	116[a]	(39)	212[b]	(49)	377[c]	(54)	561[d]	(41)
Inferior colliculus cen/dor†	290	(60)	741[a]	(109)	888[a]	(90)	1163[a]	(168)	1405[b]	(39)	1781[c]	(25)

TABLE 1. (*continued*).

Brain region	Experimental group											
	Naive		60 dB		70 dB		80 dB		90 dB		105 dB	
Inferior colliculus external†	56	(8.3)	82	(18)	171[b]	(19)	212[b]	(19)	387[c]	(42)	686[d]	(55)
Nuc lateral lemniscus†	13	(1.5)	18	(3.9)	39[b]	(2.8)	79[b]	(9.2)	171[c]	(58)	480[e]	(15)
Superior olivary complex†	26	(2.4)	63[a]	(11)	108[a]	(6.1)	147[b]	(22)	281[d]	(60)	390[d]	(15)
Locus coeruleus†	0.2	(0)	1.6[a]	(0.3)	1.6[a]	(0.3)	1.3[a]	(0.2)	3.6[a]	(1.5)	6.9[a]	(2.1)
Raphe dorsal†	2.7	(0.8)	8.8	(5.7)	7.6	(3.5)	7.9	(2.4)	23[a]	(5.0)	16	(5.1)
Raphe medial†	2.0	(0.7)	7.2	(3.1)	7.9[a]	(1.7)	6.5	(3.6)	31[d]	(6.4)	23[a]	(4.6)
Superior colliculus†	60	(15)	209[a]	(59)	293[a]	(71)	123	(27)	527[b]	(100)	294[a]	(16)
Dorsal tegmental nuc†	4.3	(2.1)	18	(4.7)	22	(11)	15	(5.7)	28[a]	(4.3)	29[a]	(4.2)
Laterodorsal teg nuc†	1.9	(0.4)	6.8	(2.0)	14[a]	(5.6)	10[a]	(0.9)	31[b]	(14)	32[b]	(4.7)
Pedunculopontine teg nuc†	5.9	(1.1)	28[a]	(5.9)	31[a]	(3.2)	32[a]	(7.3)	90[d]	(27)	63[a]	(6.5)
Ventral tegmental nuc†	6.7	(1.3)	9.9	(2.0)	14	(3.5)	16	(2.8)	31[b]	(7.0)	26[a]	(1.1)
Ventral tegmental area†	5.9	(2.9)	51[a]	(17)	46[a]	(9.3)	50[a]	(12)	89[a]	(8.6)	127[a]	(30)
Cerebellum												
Lobules (1–10)†	117	(30)	3586[a]	(985)	3750[a]	(1362)	1753[a]	(406)	5026[a]	(1106)	3259[a]	(646)
Flocculus and paraflocculus†	58	(16)	876[a]	(213)	1426[a]	(179)	2370[b]	(180)	2801[b]	(263)	2046[b]	(169)

†One-way ANOVA $P \leqslant 0.05$. Tukey Multiple Mean Comparisons: $P < 0.05$ *vs* Naive group[a]: $P < 0.05$ *vs* Naive and 60 dB Groups[b]; $P < 0.05$ *vs* Naive, 60 and 70 dB groups[c]; $P < 0.05$ *vs* Naive, 60, 70 and 80 dB groups[d]; $P < 0.05$ *vs* all other groups[e].

repeatedly exposed (10 days total) to the same experimental environment (60 dB background noise condition). A quantitatively similar induction pattern was observed in rats exposed to moderate noise increments (10 and 20 dB above background, in the 70 and 80 dB conditions, respectively), with higher induction in some auditory-related structures of rats from the 80 dB condition. This wide regional c-*fos* induction in rats exhibiting mild or no corticosterone and behavioural stress responses is perhaps reflective of processes associated with exploration induced by transferring rats from their home cages to the experimental environment, differing in shape, sound, illumination and smell. Alternatively, it is possible that the transfer from the home cage to the experimental apparatus was still mildly stressful, producing corticosterone release that could have returned to low levels 60 min after the transfer. Such a mild stress might have induced feedback inhibition that prevented corticosterone release to moderate noise intensities. Either way, this wide regional c-*fos* induction was not specific to audiogenic stress, and it is therefore possible that some of the c-*fos* induction previously reported with other stress conditions (both physical or psychological), particularly in the amygdala, thalamus and cortex, was also evoked non-specifically, even in animals repeatedly exposed to the experimental environment (1, 7, 9–11, 13, 14, 25). Because of this, it cannot be ruled out that some of the regional c-*fos* activation obtained by simply transferring rats in the experimental cage might have masked their specific involvement in audiogenic stress. The lack of difference in c-*fos* induction between rats displaying longer sleep duration compared to the lower auditory stimulation condition (60 dB background) might be explained by the delayed latency for this behaviour to occur in the session, which might have precluded the observation of peak induction of c-*fos* mRNA at the time of sacrifice (less than 30 min) associated with this specific behaviour.

c-*fos* induction above and beyond that obtained in the moderate noise conditions was observed in some brain regions of rats exposed to the loudest noise intensities (90 and 105 dB). The bed nucleus of the stria terminalis, especially its medial and ventral nuclei, the septohypothalamic nucleus, the ventral portion of the dentate gyrus, a number of hypothalamic nuclei including the lateral preoptic area, the medial preoptic nucleus and the paraventricular nucleus, the median raphe and the pedunculopontine tegmental nucleus showed particularly strong c-*fos* induction in one or both stressed groups. These regions can therefore be proposed to be part of a specific brain circuit involved in some aspects of stress responsiveness to loud auditory stimulation. In fact, a general role of some hypothalamic regions (besides the paraventricular nucleus), the bed nucleus of the stria terminalis, the septohypothalamic/ventral lateral septal area and the raphe in stress responsiveness is suggested because these regions exhibit c-*fos* induction in response to other stimuli including hypertonic saline, swim and restraint (4, 11, 12, 14, 26). Activation of the pedunculopontine tegmental nucleus and the ventral dentate gyrus has not been reported with other types of stimuli, and might therefore be specific to audiogenic stress.

The first aspect of stress responsiveness to loud auditory stimulation is the reception and transmission of the acoustic signal, which was clearly exhibited by the relationship obtained between noise intensity and c-*fos* induction in a number of auditory structures. c-*fos* induction in auditory nuclei appears to be specific to audiogenic stress, as activation of these regions has not been reported with other stressors. Although no attempts were made to determine precisely the auditory subnuclei activated with increasing noise intensities, the associated and unaligned sensory nuclei as compared to the main sensory nuclei of the auditory pathway appeared selectively active with the louder noises, as indicated by the reliably higher c-*fos* induction in the external nucleus of the inferior colliculus and the medial division of the medial geniculate body (27). The unreliable noise intensity relationship observed in the ventral/dorsal divisions of the medial geniculate body and auditory cortex might be related to a higher percentage of cells displaying non-monotonicity of rate/intensity level functions in these areas, compared to structures in the lower auditory system (28).

On the other hand, a major component involved in stress responsiveness to loud noise stimulation was the neuroendocrine (corticosterone) response which was directly associated with

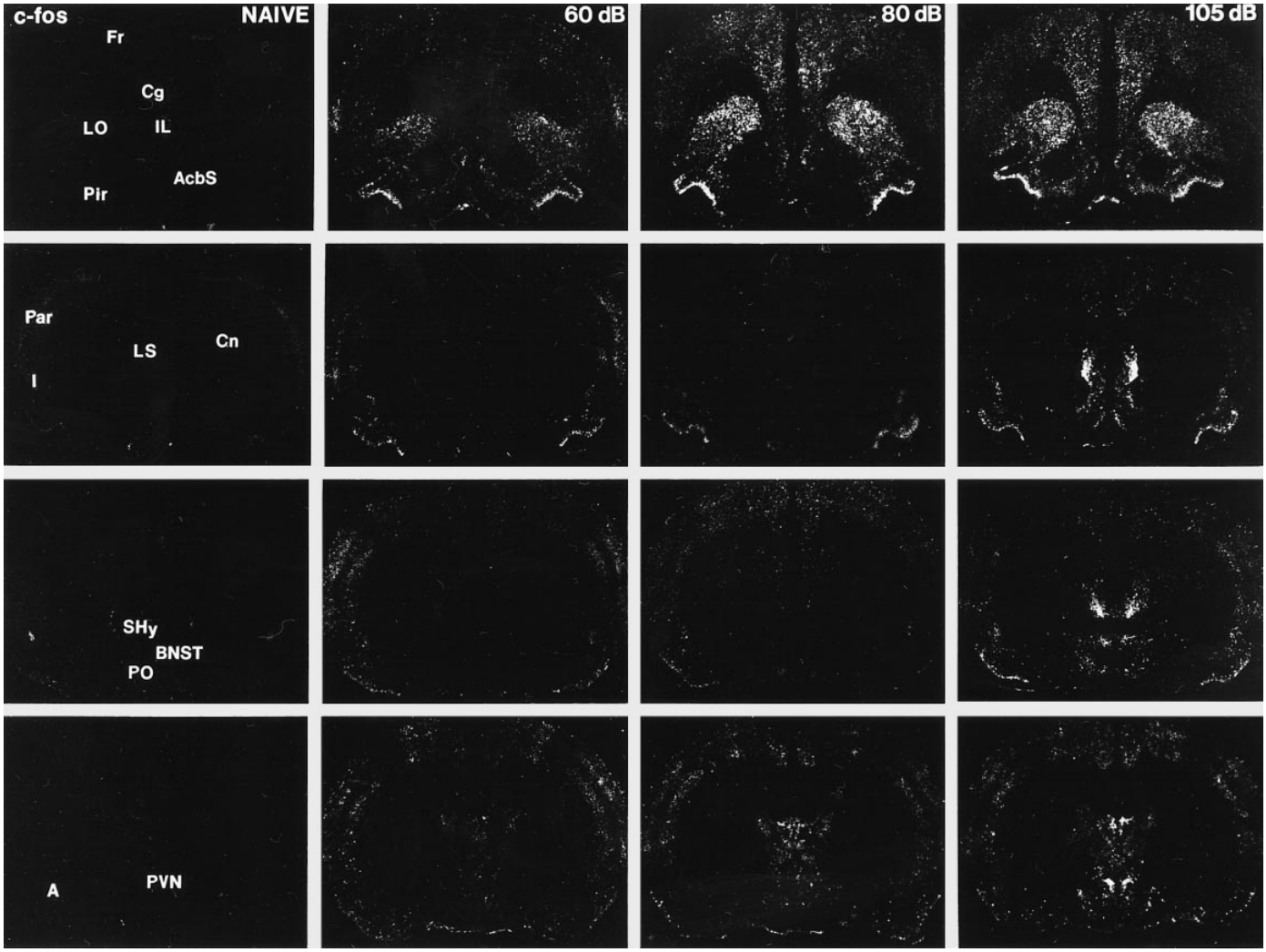

FIG. 3. Photomicrographs from x-ray films exposed for five days following *in situ* hybridization with an antisense cRNA probe against c-*fos* mRNA. Animal brain sections from Naive, 60, 80, or 105 dB conditions are represented at four different levels in the forebrain and diencephalon. Intense c-*fos* induction is observed in the bed nucleus of the stria terminalis (BNST), ventral lateral septum (LS), septohypothalamic nucleus (SHy), preoptic area (PO), and paraventricular hypothalamic nucleus (PVN) of rats in the 105 dB condition. Other abbreviations: A, amygdala; AcbS, accumbens, shell; Cg, cingulate cortex; Cn, caudate nucleus; Fr, frontal cortex; I, insular cortex; IL, infralimbic cortex; LO, lateralorbital cortex; Par, parietal cortex; Pir, piriform cortex.

strong c-*fos* induction in the parvocellular region of the paraventricular nucleus of the hypothalamus in rats exposed to the two higher noise intensities. Neurons of the parvocellular region contain corticotropin-releasing hormone and form the origin of the 'final common path' for activation of the hypothalamo-pituitary-adrenal axis, ultimately responsible for the release of corticosteroids by the adrenal cortex (29, 30). Induction of c-*fos* in the paraventricular nucleus is common to most stressors studied (4–7, 9–12, 14, 26).

Because no direct projections have been reported from auditory structures to the hypothalamic paraventricular nucleus, additional relays are required to activate CRH paraventricular neurons by audiogenic stress. Activated structures, particularly those of the hypothalamus (medial preoptic nucleus, lateral preoptic area and supramammillary nucleus) and the anterior bed nucleus of the stria terminalis are known to have direct projections to the parvocellular region of the paraventricular nucleus (26, 31–35), and are thus in a position to relay signals initiated by loud noise stimulation. In turn, the septohypothalamic nucleus and closely associated ventral lateral septum project to some of the same hypothalamic (preoptic and supramammillary nuclei) and stria terminalis areas which directly innervate the paraventricular nucleus (36). By far the heaviest projections to the anterior bed nucleus of the stria terminalis and the ventral lateral septum are from various divisions of the amygdala (36, 37). Generally, activation of the amygdala was moderate in all noise conditions, but the lateral nucleus of the amygdala showed significant c-*fos* induction in the 105 dB condition (with a trend in the 90 dB condition, $P = 0.08$) compared to the 60 dB background noise condition. The lateral nucleus projects to several basolateral and medial amygdaloid nuclei (38, 39), and is in turn innervated by the medial division of the medial geniculate nucleus (40, 41), the last auditory structure to show reliable c-*fos* induction in the stressed groups of the present study. Recently, we found that

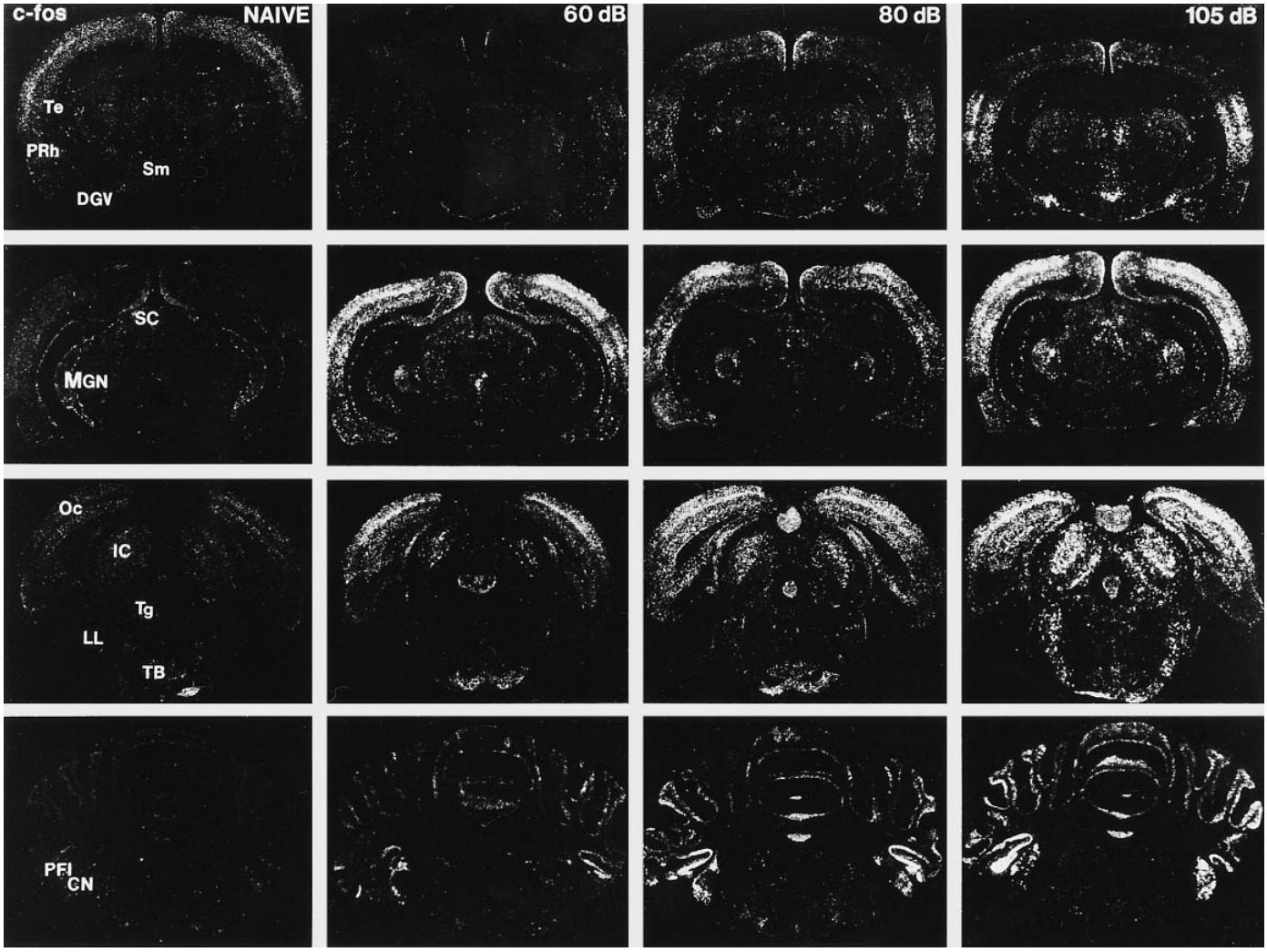

FIG. 4. Photomicrographs from x-ray films exposed for five days following *in situ* hybridization with an antisense cRNA probe against c-*fos* mRNA. Animal brain sections from Naive, 60, 80, or 105 dB conditions are represented at midbrain, pons and brainstem levels. c-*fos* induction was particularly strong and consistent in the ventral dentate gyrus (DGV), supramammillary nucleus (Sm), medial geniculate nucleus (MGN), inferior colliculus (IC), nuclei of the lateral lemniscus (LL), tegmental nuclei (Tg) and the cochlear nuclei (CN). Other abbreviations: Oc, occipital (visual) cortex; PFl, cerebellar flocculus and paraflocculus; PRh, perirhinal cortex; SC, superior colliculus; TB, trapezoid bodies; Te, auditory cortex.

neurotoxic lesions aimed at the lateral nucleus of the amygdala significantly attenuated the behavioural and neuroendocrine responses to audiogenic stress (Campeau and Watson, unpublished observations). Thus, although incomplete, the data suggest that the lateral nucleus of the amygdala might act as an interface between the auditory system and the stress responsive areas of the lateral septum and bed nucleus of the stria terminalis. The difficulty to discern clearly between different subnuclei of the medial and basolateral nuclei of the amygdala might have precluded the finding of reliable induction in some of these areas. A diagram of a putative circuit associated with audiogenic stress responsiveness is presented in Fig. 8.

Interactions of brainstem and pontine auditory areas with other brainstem regions (raphe, pedunculopontine tegmental area or other areas not investigated in the present study) could play an important role by directly innervating hypothalamic, bed nucleus of the stria terminalis or lateral septal areas. However, the results of recent studies showing complete abolition of corticosterone release specifically to audiogenic stress by complete auditory thalamic lesions (42), makes this possibility unlikely. It is possible that the activation observed in the tegmental nuclei (pedunculopontine, laterodorsal) and the lateroventral central gray is associated with the behavioural outcome of audiogenic stress. Clearly, additional studies, including lesion or inactivation procedures, will be required to determine more precisely the role of the stress responsive areas found in the present study in the neuroendocrine and behavioural responses evoked by audiogenic stress.

Materials and methods

Subjects

Twenty-four naive male albino Sprague-Dawley rats weighing 250–300 gm (Charles River Co., Kingston, NY, USA) were used. They were housed in plastic cages ($20 \times 25 \times 50$ cm) in groups of 2 with water and laboratory chow continuously available. All rats were maintained on a 12 h : 12 h

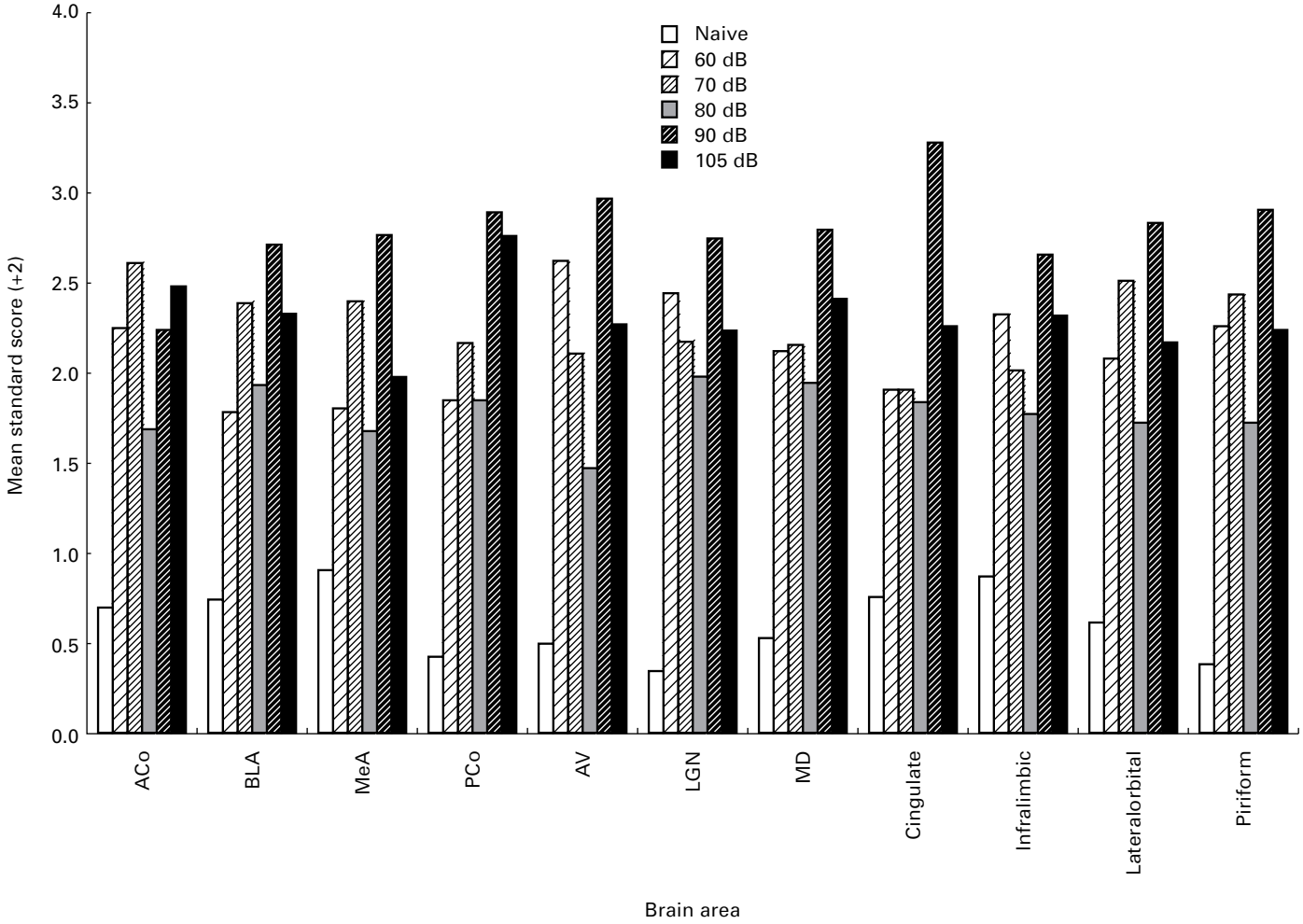

FIG. 5. Standardized c-*fos* induction in some amygdaloid, thalamic and cortical structures which was higher in all conditions compared to Naive, but not different from each other. Mean c-*fos* integrated densities were transformed to standard scores and 2 was added to all means to obtain positive values (all standard deviations have units of one). Abbreviations: ACo, anterior cortical nucleus of the amygdala; AV, anteroventral thalamic nucleus; BLA, basolateral nucleus of the amygdala; LGN, lateral geniculate nucleus; MD, mediodorsal thalamic nucleus; MeA, medial nucleus of the amygdala; PCo, posterior cortical nucleus of the amygdala.

light-dark cycle (lights on at 7.00) and acclimated to the colony rooms for a week before the experiments began. The background noise level in the quiet animal colony was ≈50 dB (A). All procedures were carried out between 7.00 and 13.00.

Apparatus

The two experimental cages were identical 20 × 25 × 30 cm Plexiglas boxes with stainless steel rod floors (2 mm bars spaced 1.2 cm apart, centre to centre). The boxes were enclosed into a ventilated, dimly lit (20 W incandescent bulb), sound attenuating LeHigh Valley chamber (53 × 56 × 96 cm). White noise (0–20 kHz) was delivered through a Grass AM7 Audio Monitor speaker, which was placed in between, and adjacent to the two boxes. The noise was produced by a General Radio Random-Noise Generator (Type 1390-A). Noise intensity was measured by placing a Radio Shack Realistic Sound Level Meter (A scale; no. 33–2050) in the boxes with the lid closed. The noise level provided by the LeHigh Valley chamber's fan and the white noise generator was ≈60 dB, which will be referred here as the background noise level of the experimental cages.

Behavioural procedures

The rats were handled for 3 to 4 min and placed in the experimental cages for 10 min daily for 9 consecutive days. Twenty-four or 48 h later, the rats were placed in the experimental boxes for 60 min. For the last 30 min, white noise of either 60 dB (background noise; no change), 70 dB, 80 dB, 90 dB, or 105 dB were presented to different groups of rats (n = 4/group). During the 30 min white noise presentation, the behaviour of all rats was scored every 10 s in one of the following 5 categories: immobility (freezing posture or sitting posture with head up and no detectable movement except for breathing), grooming, locomoting, rearing, and sleeping (characteristic curled position with tail under body and head on the floor). The rats were then immediately decapitated following noise exposure, trunk blood was collected and the brains were rapidly removed and frozen in chilled isopentane (−40 °C). Four rats that were not handled or exposed to the experimental boxes served as naive controls and were decapitated immediately upon removal from the colony room.

Corticosterone radioimmunoassay

Upon decapitation, trunk blood was collected into ice chilled tubes containing EDTA. Blood samples were centrifuged at 1500 *g* for 10 min, the plasma was pipetted into 0.5 ml Ependorf microcentrifuge tubes, and stored at −20 °C until assayed.

Corticosterone was measured by radioimmunoassay using a specific rabbit antibody raised in our laboratory, with less than 3% crossreactivity with other steroids, including cortisol, deoxycorticosterone, aldosterone, testosterone and progesterone (Dr Dana Helmreich, personal communication). Plasma samples were diluted 1 : 100 in 0.05 M sodium phosphate buffer containing 0.25% bovine serum albumin (BSA) pH 7.4, and corticosterone separated from binding protein by heat (70 °C, 30 min).

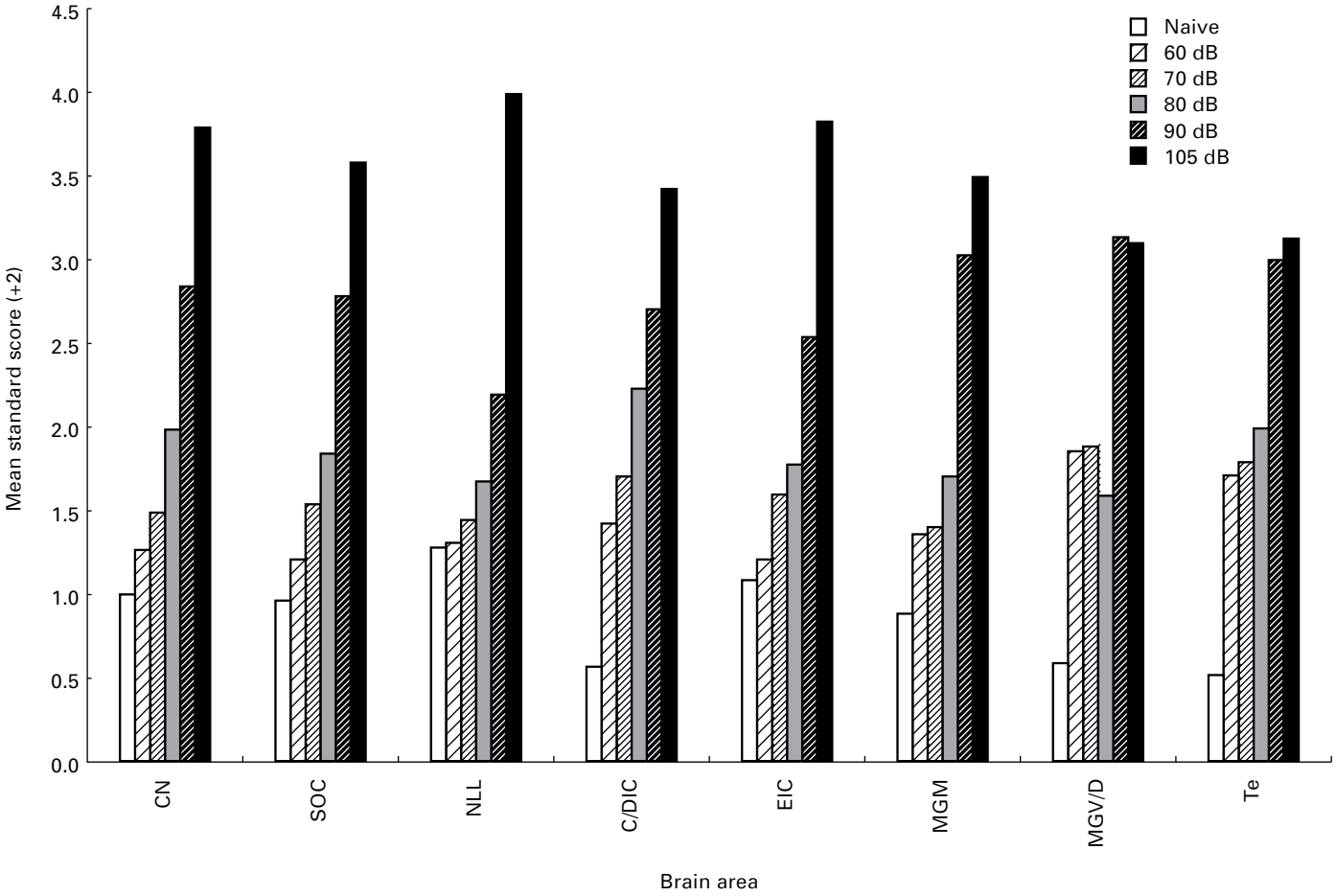

FIG. 6. Standardized c-*fos* induction show an intensity dependent c-*fos* induction in many auditory regions. Mean integrated c-*fos* densities were transformed to standard scores and 2 was added to all means to obtain positive values (all standard deviations have units of one). Abbreviations: CN, cochlear nuclei; C/DIC, central/dorsal nuclei of the inferior colliculus; EIC, external nucleus of the inferior colliculus; MGM, medial division of the medial geniculate nucleus; MGV/D, ventral and dorsal divisions of the medial geniculate nucleus; NLL, nuclei of the lateral lemniscus; SOC, superior olivary complex; Te, auditory cortex.

Duplicate samples of 200 µl to which 50 µl of trace (^{3}H-corticosterone; Amersham 50 Ci/mmol, 10,000 cpm/tube) and 50 µl of antibody (final concentration 1 : 12800) were incubated at 4 °C overnight. Separation of bound from free corticosterone was achieved by adding 0.5 ml of chilled 1% charcoal–0.1% dextran mixture in buffer for 10 min at 4 °C and centrifuged for 10 min at 3000 rpm. (Sorvall RC-5B). The supernatant was poured into 4 ml scintillation fluid and bound ^{3}H-corticosterone counted on a Packard CA2000 liquid scintillation analyzer and compared to a standard curve (range: 0–80 µg/dl). All samples were measured simultaneously to reduce interassay variability; within assay variability was less than 5%.

In situ *hybridization histochemistry*

After rapid decapitation, brains were removed and frozen in isopentane chilled to −40° to −50 °C, and stored at −80 °C. Ten micron sections were then cut on a Bright cryostat, thaw mounted onto polylysine coated slides, and stored at −80 °C until further processed. Slides were fixed in a buffered 4% paraformaldehyde solution for 1 h. Tissue sections were then deproteinated with Proteinase K (1.0 µg/ml) for 10 min at 37 °C. The slides were then rinsed in H_2O for 5 min, acetylated in 0.1 M triethanolamine containing 0.25% acetic anhydride for 10 min, rinsed for an additional 5 min in H_2O, and dehydrated in a progressive series of alcohols.

^{35}S-labelled cRNA probes were generated for c-*fos* from cDNA subclones in transcription vectors using standard *in vitro* transcription methodology. The rat c-*fos* cDNA clone (courtesy of Dr T. Curran) was subcloned in pGem3Z (courtesy of Dr C. A. Fox) and cut with HindIII to yield a 680 nt cRNA probe. Riboprobes were labelled in a reaction mixture consisting of 1 µg linearized plasmid, 1X T7 or SP6 transcription buffer (BRL), 125 µCi ^{35}S-UTP, 150 µM NTPs-UTP, 12.5 mM dithiothreitol, 20 U RNase inhibitor, and 6 U polymerase. The reaction was allowed to proceed for 120 min at 37 °C, and probe was separated from free nucleotides over a Sephadex G50–50 column. Riboprobes were diluted in hybridization buffer to yield $\approx 1.5 \times 10^6$ dpm/30 µl buffer. The hybridization buffer consisted of 50% formamide, 10% dextran sulfate, 3 × SSC, 50 mM sodium phosphate buffer (pH = 7.4), 1X Denhardt's solution, and 0.1 mg/ml yeast tRNA. Diluted probe (30 µl) was applied to each slide and sections were coverslipped. Slides were placed in sealed plastic boxes lined with filter paper moistened with 50% formamide in 50 mM sodium phosphate buffer, and were subsequently incubated for 12 h at 55 °C. Coverslips were then removed, and slides were rinsed several times in 2 × SSC. Slides were then incubated in RNase A (200 µg/ml) for 60 min. at 37 °C, washed successively in 2X, 1X, 0.5X and 0.1 × SSC for 5–10 min each, and washed in 0.1 × SSC for 60 min. at 65 °C. Slides were subsequently rinsed in fresh 0.1 × SSC, dehydrated in a graded series of alcohols, and exposed to Kodak XAR X-ray film.

Control experiments were performed on tissue sections pre-treated with RNase A (200 µg/ml at 37 °C for 60 min.) prior to hybridization; this treatment prevented labelling. Alternatively, some control sections were hybridized with the sense cRNA strands, which in all cases did not lead to significant hybridization to tissue sections.

Importantly, three to five slides for a given brain region from each rat

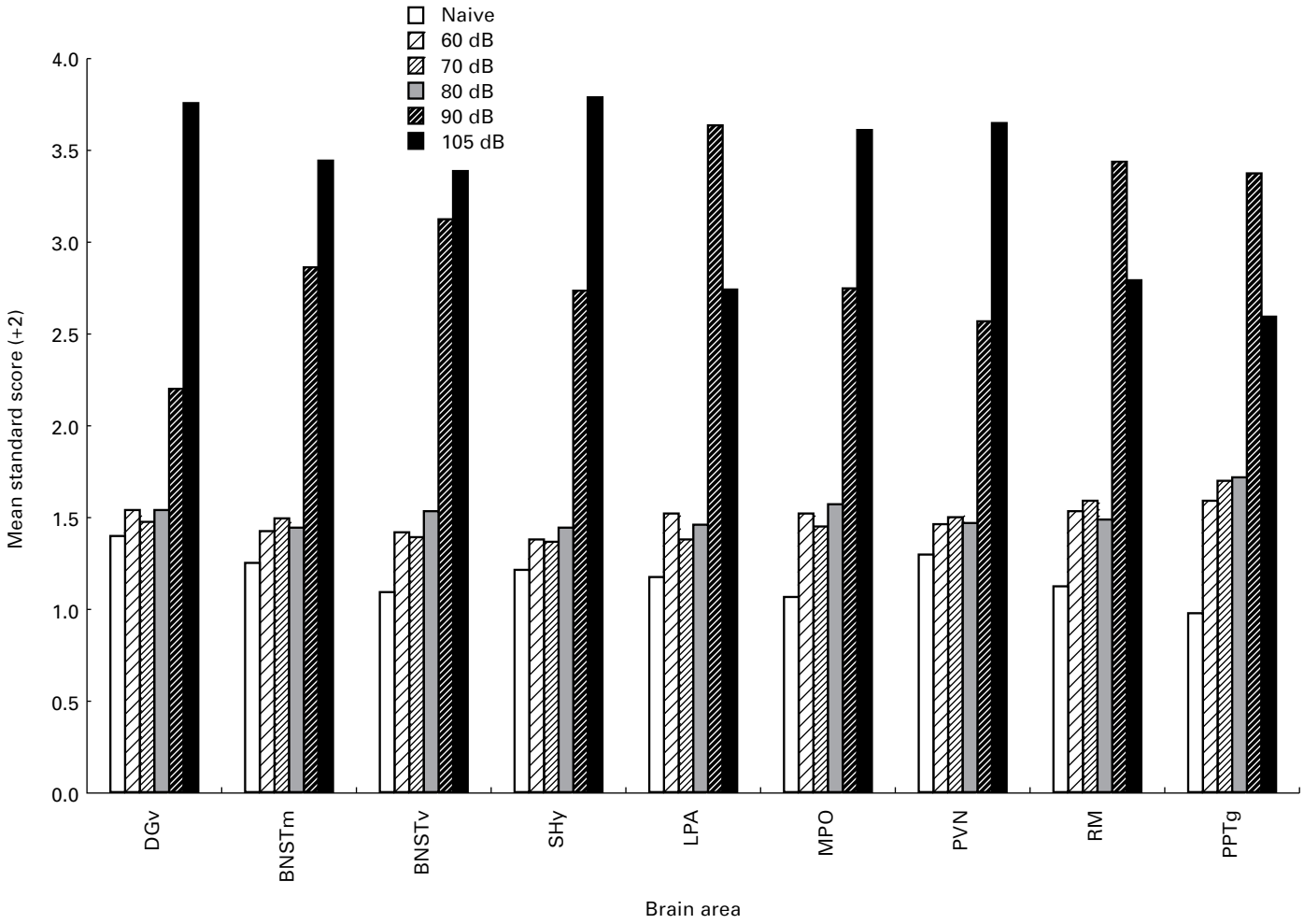

FIG. 7. Standardized c-*fos* induction in regions where the 90 and/or 105 dB conditions produced reliable induction compared to all other conditions. Mean integrated c-*fos* densities were transformed to standard scores and 2 was added to all means to obtain positive values (all standard deviations have units of one). Abbreviations: BNSTm, medial nucleus of the bed nucleus of the stria terminalis; BNSTv, ventral nucleus of the bed nucleus of the stria terminalis; DGv, ventral dentate gyrus; LPA, lateral preoptic area; MPO, medial preoptic nucleus; PPTg, pedunculopontine tegmental nucleus; PVN, paraventricular nucleus of the hypothalamus; RM, median raphe; SHy, septohypothalamic nucleus.

included in the study were processed simultaneously to allow direct comparisons in the same regions. Multiple *in situ* hybridizations were thus performed at different levels of the brain with all animals represented to reduce the effects of technical variations within regions. Sections of all rats in the same region were all exposed on the same x-ray film to further minimize variations. Semi-quantitative analyses were performed on digitized images from x-ray films in the linear range of the gray values obtained from our acquisition system (Northern Light lightbox model B 95, a Pulnix TV camera model TM-745 fitted with a Nikkor 55 mm lens, connected to an A/D converter onboard a Macintosh Quadra 840AV, captured with NIH Image v1.59). Signal pixels of a region of interest were defined as being 3.5 standard deviations above the mean of a cell poor area close to the region of interest. The number of pixels and the average pixel values above the set background were then computed for each regions of interest, and multiplied, giving an integrated densitometric measure. An average of 4 to 6 measurements were made on different sections, for each region of interest, and these values were further averaged to get a single integrated density value per region for each rat. Slides undergoing *in situ* hybridization were stained with cresyl violet and used extensively in the determination of regional boundaries on the digitized images.

Statistics

Repeated measures analysis of variance (ANOVA) was performed on the means of each behavioural categories in separate 5-min periods. Additional one-way ANOVAs were performed at each time period if an overall Condition or Condition × Time period effect were initially detected, to determine more precisely the source of significant effects, with Tukey's multiple mean comparisons following significant ANOVAs. One-way ANOVA was performed on plasma corticosterone levels, followed by a Tukey multiple mean comparison test to determine the source of significant effects.

For purposes of statistical analysis, the mean c-*fos* integrated density values were transformed to natural logarithm values to reduce between group variances observed in some regions. One-way ANOVAs were performed on the transformed mean integrated densities obtained from each region where c-*fos* mRNA induction was measured. This was followed by Tukey's post-hoc multiple mean comparisons to determine more exactly the source of the differences obtained with the initial ANOVA. Statistical significance in all instances was set to $P = 0.05$.

Acknowledgements

This research was supported by NIMH Grant MH-42251 (S.J.W.), and a Postdoctoral Fellowship from the Medical Research Council of Canada (S.C). Thanks are extended to Dr Heidi E.W. Day for critical comments on an earlier draft of this manuscript.

Accepted 21 January 1997

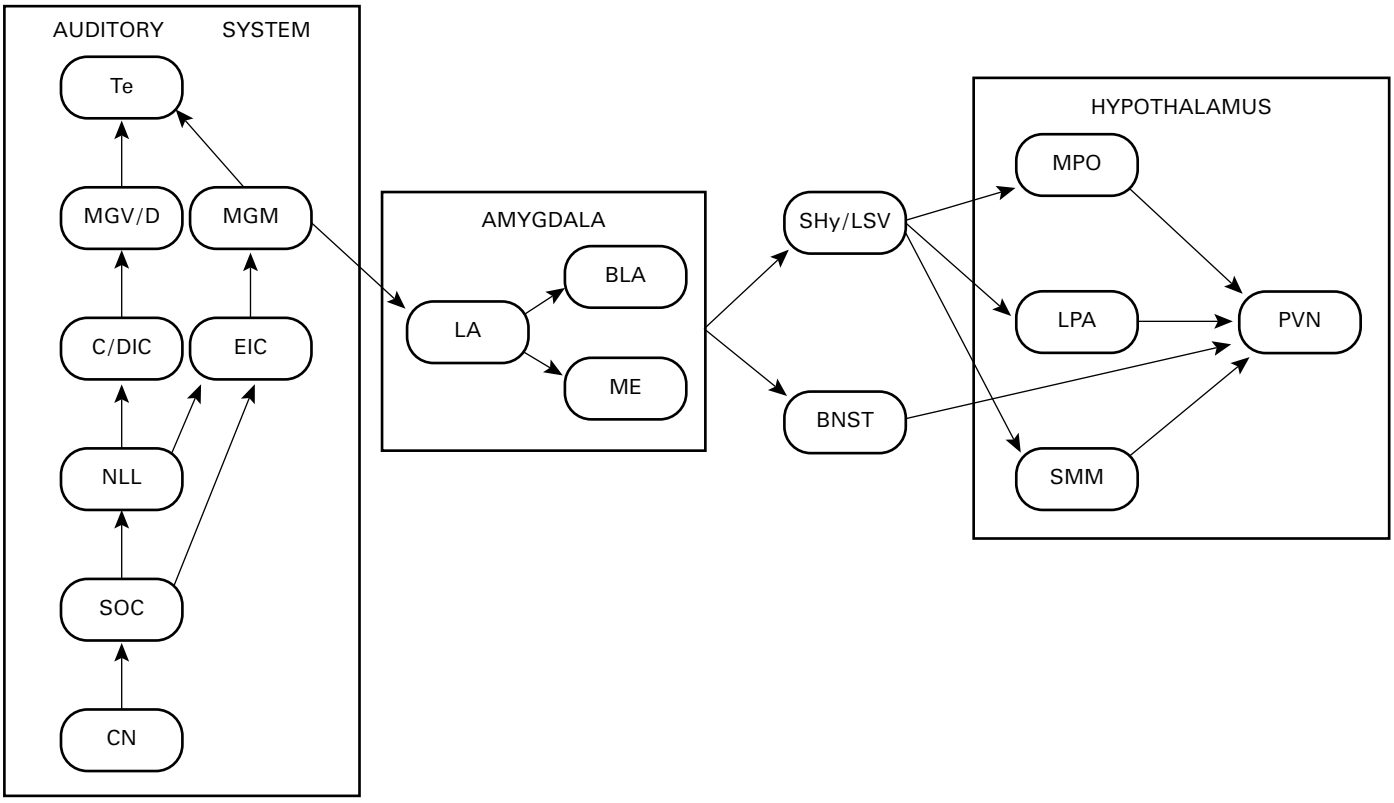

FIG. 8. Schematic diagram of a putative circuit involved in activation of CRH containing neurons of the paraventricular hypothalamic nucleus by audiogenic stress. Arrows indicate known projections between the various areas illustrated, but are not exclusive. Abbreviations: Auditory system, CN, cochlear nuclei; SOC, superior olivary complex; NLL, nuclei of the lateral lemniscus; C/DIC, central/dorsal nuclei of the inferior colliculus; EIC, external nucleus of the inferior colliculus; MGV/D, ventral and dorsal divisions of the medial geniculate body; MGM, medial division of the medial geniculate body; Te, auditory cortex; Amygdala, LA, lateral nucleus; BLA, basolateral nucleus; ME, medial nucleus; BNST, bed nucleus of the stria terminalis; SHy/LSV, septohypothalamic nucleus/ventral lateral septum; Hypothalamus, MPO, medial preoptic nucleus; LPA, lateral preoptic area; SMM, supramammillary nucleus; PVN, paraventricular nucleus.

References

1 Beck CHM, Fibiger HC. Conditioned fear-induced changes in behavior and in the expression of the immediate early gene c-fos: With and without diazepam pretreatment. *J Neurosci* 1995; **15**: 709–720.

2 Campeau S, Hayward M, Hope B *et al.* Induction of the c-*fos* proto-oncogene in the rat amygdala during unconditioned and conditioned fear. *Brain Res* 1991; **565**: 349–352.

3 Schreiber SS, Tocco G, Shors TJ *et al.* Activation of immediate early genes after acute stress. *NeuroReport* 1991; **2**: 17–20.

4 Sharp F, Sagar S, Hicks K *et al.* c-fos mRNA, Fos and Fos-related antigen induction by hypertonic saline and stress. *J Neurosci* 1991; **11**: 2321–2331.

5 Arnold F, De Lucas Bueno M, Shiers H *et al.* Expression of c-fos in regions of the basal limbic forebrain following intracerebroventricular corticotropin-releasing factor in unstressed and stressed male rats. *Neuroscience* 1992; **51**: 377–390.

6 Smith MA, Banerjee S, Gold PW *et al.* Induction of c-*fos* mRNA in rat brain by conditioned and unconditioned stressors. *Brain Res* 1992; **578**: 135–141.

7 Pezzone M, Lee W-S, Hoffman G *et al.* Induction of c-Fos immunoreactivity in the rat forebrain by conditioned and unconditioned aversive stimuli. *Brain Res* 1992; **597**: 41–50.

8 Pezzone M, Lee W-S, Hoffman G *et al.* Activation of brainstem catecholaminergic neurons by conditioned and unconditioned aversive stimuli as revealed by c-Fos immunoreactivity. *Brain Res* 1993; **608**: 310–318.

9 Senba E, Matsunaga K, Tohyama M *et al.* Stress-induced c-fos expression in the rat brain: activation mechanism of sympathetic pathway. *Brain Res Bull* 1993; **31**: 329–344.

10 Duncan G, Johnson K, Breese G. Topographic patterns of brain activity in response to swim stress: assesment by 2-deoxyglucose uptake and expression of Fos-like immunoreactivity. *J Neurosci* 1993; **13**: 3932–3943.

11 Duncan G, Knapp D, Breese G. Neuroanatomical characterization of Fos induction in rat behavioral models of anxiety. *Brain Res* 1996; **713**: 79–91.

12 Bonaz B, Tache Y. Induction of Fos immunoreactivity in the rat brain after cold- restraint induced gastric lesions and fecal excretion. *Brain Res* 1994; **652**: 56–64.

13 Melia KR, Ryabinin AE, Schroeder R *et al.* Induction and habituation of immediate early gene expression in rat brain by acute and repeated restraint stress. *J Neurosci* 1994; **14**: 5929–5938.

14 Cullinan WE, Herman JP, Battaglia DF *et al* Pattern and time course of immediate early gene expression in rat brain following acute stress. *Neuroscience* 1995; **64**: 477–505.

15 Henkin RI, Knigge KM. Effect of sound on the hypothalamic-pituitary-adrenal axis. *Am J Physiol* 1963; **204**: 910–914.

16 Collu R, Jequier JC. Pituitary response to auditory stress: Effects of treatment with a-methyl-p-tyrosine. Usefulness of a factorial mixed design for statistical analysis. *Can J Physiol Pharmacol* 1976; **54**: 596–602.

17 Borrell J, Torrellas A, Guaza C *et al.* Sound stimulation and its effects on the pituitary-adrenocortical function and brain catecholamines in rats. *Neuroendocrinology* 1980; **31**: 53–59.

18 Armario A, Castellanos J, Balasch J. Adaptation of anterior pituitary hormones to chronic noise stress in male rats. *Behav Neural Biol* 1984; **41**: 71–76.

19 Irwin MR, Segal DS, Hauger RL *et al.* Individual behavioral and neuroendocrine differences in responsiveness to audiogenic stress. *Pharmacol Biochem Behav* 1989; **32**: 913–917.
20 Segal DS, Kuczenski R, Swick D. Audiogenic stress response: behavioral characteristics and underlying monoamine mechanisms. *J Neural Transm* 1989; **75**: 31–50.
21 Britton KT, Segal DS, Kuczenski R *et al.* Dissociation between *in vivo* hippocampal norepinephrine response and behavioral/neuroendocrine responses to noise stress in rats. *Brain Res* 1992; **574**: 125–130.
22 Spencer JAD, Moran DJ, Lee A *et al.* White noise and sleep induction. *Arch Dis Child* 1990; **65**: 135–137.
23 Arankowsky-Sandoval G, Stone WS, Gold PE. Enhancement of REM sleep with auditory stimulation in young and old rats. *Brain Res* 1992; **589**: 353–357.
24 Kawada T, Suzuki S. Sleep induction effects of steady 60 dB (A) pink noise. *Ind Health* 1993; **31**: 35–38.
25 Smith C, Hauser E, Renaud N *et al.* Increased hypothalamic [3H]flunitrazepam binding in hypothalamic-pituitary-adrenal axis hyporesponsive Lewis rats. *Brain Res* 1992; **569**: 295–299.
26 Cullinan W, Helmreich D, Watson S. Fos expression in forebrain afferents to the hypothalamic paraventricular nucleus following swim stress. *J Comp Neurol* 1996; **368**: 88–99.
27 Winer JA, Morest DK. The medial division of the medial geniculate body of the cat: Implications for thalamic organization. *J Neurosci* 1983; **3**: 2629–2651.
28 Aitkin L. *The Auditory Cortex: Structural and functional bases of auditory perception*. London: Chapman and Hall, 1990.
29 Sawchenko PE. The final common path: Issues concerning the organization of central mechanisms controlling corticotropin secretion. In: Brown M, Koob G, Rivier C, eds. *Stress Neurobiology and Neuroendocrinology* New York: Marcel Dekker, 1991 55–71.
30 Akil H, Morano M. Stress. In: Bloom F, Kupfer D, eds. *Psychopharmacology: The Fourth Generation of Progress.* New York: Raven Press, Ltd, 1995 773–785.
31 Simerly RB, Swanson LW. Projections of the medial preoptic nucleus: A *Phaseolus vulgaris* leucoagglutinin anterograde tract-tracing study in the rat. *J Comp Neurol* 1988; **270**: 209–242.
32 Vertes RP. PHA-L analysis of projections from the supramammillary nucleus in the rat. *J Comp Neurol* 1992; **326**: 595–622.
33 Cullinan WE, Herman JP, Watson SJ. Ventral subicular interaction with the hypothalamic paraventricular nucleus: evidence for a relay in the bed nucleus of the stria terminalis. *J Comp Neurol* 1993; **332**: 1–20.
34 Moga M, Saper C. Neuropeptide-immunoreactive neurons projecting to the paraventricular hypothalamic nucleus in the rat. *J Comp Neurol* 1994; **346**: 137–150.
35 Sawchenko PE, Swanson LW. The organization of the forebrain afferents to the paraventricular and supraoptic nuclei. *J Comp Neurol* 1983; **218**: 121–144.
36 Swanson LW, Cowan WM. The connections of the septal region in the rat. *J Comp Neurol* 1979; **186**: 621–656.
37 Weller KL, Smith DA. Afferent connections to the bed nucleus of the stria terminalis. *Brain Res* 1982; **232**: 255–270.
38 Stefanacci L, Farb CR, Pitkanen A *et al.* Projections from the lateral nucleus to the basal nucleus of the amygdala: a light and electron microscopic PHA-L study in the rat. *J Comp Neurol* 1992; **323**: 586–601.
39 Pitkanen A, Stefanacci L, Farb CR *et al.* Intrinsic connections of the rat amygdaloid complex: projections originating in the lateral nucleus. *J Comp Neurol* 1995; **356**: 288–310.
40 LeDoux JE, Ruggiero DA, Reis DJ. Projections to the subcortical forebrain from anatomically defined regions of the medial geniculate body in the rat. *J Comp Neurol* 1985; **242**: 182–213.
41 LeDoux JE, Farb C, Ruggiero DA. Topographic organization of neurons in the acoustic thalamus that project to the amygdala. *J Neurosci* 1990; **10**: 1043–1054.
42 Campeau S, Akil H, Watson SJ. Lesions of the auditory thalamus specifically block corticosterone release and induction of c-*fos* mRNA in the forebrain associated with loud noise stress in rats. *Soc Neurosci Abstr* 1996; **22**: 1148.